Jingai Hao[1,2]

Yinfeng Zhao[1]

Mao Ye[1]

Zhongmin Liu[1]

[1]National Engineering Laboratory for MTO, iCHEM (Collaborative Innovation Center of Chemistry for Energy Materials), Dalian Institute of Chemical Physics, Chinese Academy of Sciences, Dalian, China.

[2]University of Chinese Academy of Sciences, Beijing, China.

Supporting Information
available online

Influence of Temperature on Fluidized-Bed Catalyst Attrition Behavior

Particle attrition is a prevalent problem in fluidized beds due to continuous moving of catalyst particles. It is always operated at high temperature either for lab- or industrial-scale fluidized beds. The influence of temperature on the attrition behavior of commercial methanol-to-olefins (MTO) and fluid catalytic cracking (FCC) catalysts is analyzed in a three-orifice lab-scale fluidized bed device from room temperature to 600 °C. The two catalysts are found to be alike in attrition mode. Both change from a combination of abrasion and fragmentation to main abrasion with increasing temperature, but differ greatly in the variation of attrition index with temperature which may be attributed to the difference of material and particle properties. An empirical correlation of attrition index to attrition temperature for all test samples is proposed.

1 Introduction

The gas-solid fluidized bed is an indispensable reactor type in chemical and petrochemical industries due to its various advantages such as fast mixing and heat exchange. Typical applications include fluid catalytic cracking (FCC) and methanol-to-olefins (MTO) process. The attrition of catalyst particles is a crucial issue in the operation of fluidized-bed reactors, on account of the continuous movement of the catalyst particles. Multiple-stage cyclones are common practices in both industrial FCC and MTO units, which are used to capture the fines generated during the normal operation. In industrial FCC units, multiple-stage cyclones can typically recover fines in the size range of 10–45 μm with high efficiency (> 99 %). As a recently developed process, the design of MTO fluidized-bed reactors and the internals inside borrowed a lot of experiences from FCC fluidized beds since both FCC and MTO catalyst particles are the A-type according to Geldart's classification [1]. Of particular importance are the cyclones in the MTO fluidized-bed reactors, which basically follow the design routine of those in industrial FCC fluidized beds. Note that the design of cyclones has consequences on operation cost, product quality, and environment pollution. It is critical to understand the attrition mechanism of MTO and FCC catalyst particles in fluidized-bed reactors at high temperature. This work embodies the authors' ambition in this direction.

Catalyst particle attrition in fluidized-bed reactors is complicated since it is affected by the properties of catalyst particles, such as surface morphology, shape, cracks, composition, and internal structure, the operating conditions, such as temperature, pressure, and gas velocity, and the layout of reactor internals, such as cyclones, air grid, and catalyst inlet device [2, 3]. Different operating conditions and fluidized-bed internal layout may lead to various stress types on particles. Mechanical stress plays a critical part when catalyst particles collide with each other or the inner reactor wall. Meanwhile, the uneven temperature distribution during operation will induce a thermal stress inside the particles. In the presence of chemical reactions in the reactor, there also exists chemical stress inside the catalyst particles. These stresses in the reactor can cause different attrition mechanisms of catalyst particles [2, 3].

In general, the particle attrition can be classified as either abrasion or fragmentation, mainly identified by the change of particle size distribution (PSD) before and after operations [4]. Abrasion normally occurs at the particle surface due to lateral cracks and surface wear, and is featured by the generation of a large amount of fines hard to capture by cyclones, whereas the change of PSD is negligible. Fragmentation refers to the breakdown of catalyst particles into smaller pieces with similar size. The PSD can vary significantly in the fragmentation process. In many cases both the abrasion and fragmentation may be found.

The research of attrition of FCC catalysts could go back to as early as 1949 [5] when the FCC process was still in its infancy. Since then extensive work has been devoted to the attrition of FCC catalyst particles [6–10]. It has been found that the attrition of catalyst particles in an FCC fluidized-bed reactor can come from the high-velocity jet by the air grid, bubble-induced particle motion, and cyclones [11–14]. Although the attrition

Correspondence: Prof. Mao Ye (maoye@dicp.ac.cn), National Engineering Laboratory for MTO, Dalian Institute of Chemical Physics, Chinese Academy of Sciences, 457 Zhongshan Road, Dalian, 116023, China.

of FCC catalyst particles inside fluidized beds is controlled in a complicated manner by the properties of catalyst particles, operating conditions, and layout of reactor internals, both abrasion and fragmentation are found as the attrition mechanism for FCC catalyst particles, leading to the size of fines of 10–40 µm, which is well within the optimal operation range of cyclones. However, most of these studies on catalyst attrition are performed at room temperature. Despite the catalytic reactions occur at high temperature, the physical properties of the flowing gas and particles, as well as the hydrodynamic regime in fluidized beds, vary significantly with temperature [15–17]. This indeed leads the stress distribution on the surface and inside of the particles differing from that at room temperature, and eventually affects particles' attrition behavior at high temperature. Hao et al. [18] recently studied the attrition mechanism of MTO catalyst particles at room temperature and 500 °C, and found that temperature has a substantial impact on the attrition mechanism of MTO catalyst particles.

Attrition has been studied for many materials at room temperature, e.g., Fischer-Tropsch catalyst [19–24], coal [25, 26], glass [27], oxygen carriers [3, 28–30], and various crystals [31–33]. Lin et al. [21] and Bukur et al. [20, 22] carried out the attrition tests of an iron Fischer-Tropsch (F-T) catalyst in a stirred-tank slurry reactor. They concluded that attrition of the F-T catalyst was induced by both the mechanical stress from particles' collisions and the chemical stress due to phase transformation. Lin and Wey [34, 35] studied the attrition of silica sand at high temperature in a bubble fluidized-bed incinerator. They found that prediction results from existing correlations derived at room temperature could not coincide with their experimental results achieved at high temperatures, whereas the attrition rate increased with higher temperature.

Chen et al. [36–38] investigated the attrition of limestone by impact tests in a circulating fluidized-bed combustor at temperatures from 25 °C to 850 °C. They stated that the attrition decreased with increasing temperature, which is in contrast to the findings of Lin and Wey [34, 35]. The attrition of calcium-based sorbents for removing sulfur dioxide (limestone, dolomite, lime etc.) in fluidized-bed combustors has also been studied at high temperature [39, 40]. Li et al. [41] examined the attrition of silica sand and petroleum coke in a hot fluidized bed with an attrition nozzle operating at temperatures from ambient to 500 °C. They concluded that the dominant attrition mechanism at high temperature is fragmentation and high temperature promotes particle attrition. They also showed that the petroleum coke produced fines with relatively larger size after attrition at higher temperature, while the results are reverse for silica sands. Nevertheless, these results indicate that the attrition behavior at high temperature varies with experimental conditions and materials utilized.

However, the knowledge on attrition of FCC and MTO catalysts at high temperature in fluidized beds is limited. The aim of this experimental study is to explore the influence of temperature on the attrition rate of MTO and FCC catalyst particles in the temperature range from ambient to 600 °C, and to understand the attrition mechanism of MTO and FCC catalysts at high temperature, in order to shed some light on the cyclone design in industrial units.

2 Experimental

2.1 Experimental Apparatus

The experimental apparatus follows the ASTM D5757-11 [42], which is composed of a reactor and a 3-µm orifice stainless-steel distribution plate. The reactor consists of four parts: gas-preheating chamber, attrition chamber, particles settling chamber, and fines collector. The 5 mm thick distributor plate is placed inside the reactor tube, which separates the tube to the upper attrition chamber and lower gas-heating chamber. Three orifices with 0.5 mm diameter are isometric from each other and 10 mm from the center of the plate. An electric heating device that can heat the reactor up to 700 °C is installed outside the preheating and attrition chamber, as shown in Fig. 1.
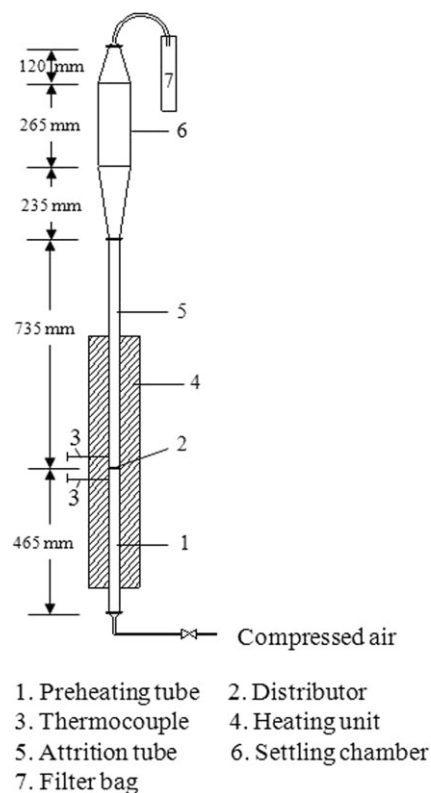
Figure 1. Air jet fluidized-bed experimental apparatus [18].

Above the attrition chamber is the particle setting chamber, which is connected to the fine collector. The stainless-steel reactor tube is 34 mm in inner diameter, and therein, the length of the gas-preheating chamber is 462 mm and of the attrition chamber 733 mm. The particles settling chamber is 620 mm in length, being cylindrical in the middle part and conical at two ends. The inner diameter of the cylindrical part is 110 mm, the lengths of the upper and lower cone are 120 mm and 235 mm, respectively, with two terminals converging to a diameter of 34 mm.

The fines collector has a filter bag that can collect fines larger than 0.1 µm and withstand up to 260 °C. The experiments were

carried out from room temperature to 600 °C with compressed air under ambient pressure.

2.2 Materials

The samples used in the experiments are listed in Tab. 1. Three different types of particles, i.e., MTO catalyst, FCC catalyst, and inert particles, were studied. The MTO catalyst and inert particles were both supplied by Chia Tai Energy Materials (Dalian) Co. Ltd. (China), the FCC-1 catalyst was from Beijing Huiersanji Green Chem Co. Ltd. (China), and the FCC-2,3 catalyst was purchased from Zibo Xinhong Chemical Co. Ltd. (China).

Table 1. Properties and mass of samples used in the experiments.

| Sample	d_{50} [μm]	$D[3,2]$ [μm]	Bulk density [g cm^{-3}]	m_0 [g]
MTO-1	117	112	0.71	50
MTO-2	124	121	0.71	100
FCC-1	116	110	0.79	50
FCC-2	126	122	0.76	100
FCC-3	126	122	0.76	200
Inert particle-1	130	127	1.03	100
Inert particle-2	130	127	1.03	200

Both the MTO and FCC catalyst are fresh industrial catalysts and are mainly composed of zeolite, binder, matrix, and additives. The inert particles have almost identical compositions as the MTO catalyst particles except SAPO-34 zeolites, which were used in the cold-flow experiments or commercial MTO units for fluidization tests before starting up. All the MTO, FCC, and inert particles were manufactured by spray-drying and then calcined at high temperature; they have not been sintered or hardened. Tab. 2 lists the compositions of MTO and FCC catalysts.

Prior to the experiments, the samples were screened by two sieves to get a narrow PSD of particles. FCC-1 and MTO-1 have a little broader PSD than the other samples. Fig. 2 shows the PSDs of the initial samples.

The PSDs were analyzed by a Malvern laser particle size analyzer (Mastersizer 2000), in which the deionized water was used to disperse the sample under ultrasonic condition prior to analysis and the morphology was determined by scanning electron microscopy (SEM; Hitachi TM 3000). Fig. 3 depicts the SEM photos of typical MTO and FCC catalysts. All samples were calcined in a muffle furnace at 600 °C for 3 h and cooled down to room temperature in vacuum desiccators before each test.

Table 2. Compositions of MTO and FCC samples.

Composition [wt %]	MTO-1, 2	FCC-1	FCC-2,3
Al_2O_3	54.02	50.38	49.46
SiO_2	25.00	40.41	41.22
P_2O_5	19.72	0.85	1.05
La_2O_3	0	4.38	4.33
SO_3	0.23	0.80	1.19
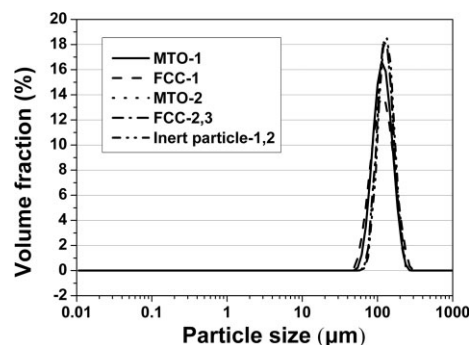
Figure 2. PSDs of initial samples.

2.3 Attrition Measurements

The experimental apparatus was first preheated to a temperature slightly lower than the desired one. Then the weighed catalyst sample was charged into the apparatus from the top of the settling chamber. Meanwhile, a gas flow of 1 L min^{-1} was blown into the fluidized bed to prevent falling of catalyst particles through the orifices of the distributor plate. The preheating and attrition chamber, when filled with particles, were further heated to the desired temperature. Then the gas flow was turned carefully to the target flow rate. The operating conditions were the same for all samples. The gas velocity through the orifices was fixed at 424 m s^{-1}, thus the superficial gas velocity in the attrition tube was set at 0.28 m s^{-1}, by altering the flow rate for different temperatures since the attrition may change with gas velocity. The test time was 12 h.
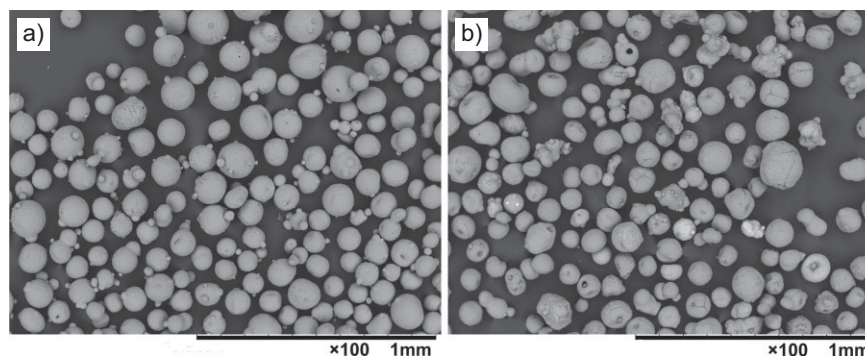
Figure 3. Typical SEM photos of initial samples: (a) MTO-1, (b) FCC-1.

In this study, the gas velocity of the orifice was much higher than that encountered in the real industrial fluidized-bed reactors. Such a high gas velocity was used in the laboratory-scale experiments in order to shorten the test time. In real units, the attrition of catalysts is related to long-term operation, i.e., several months to several years. Investigating the attrition mechanism under real operation conditions with such a long duration is extremely difficult, if not impossible. Therefore, as common practice [5, 10, 42], the attrition of catalysts was normally tested in laboratory facilities with a much higher gas velocity but within a relatively short time.

During the tests, elutriated fine particles were collected by the filter bags, which should be replaced quickly at a predetermined time interval. The filter bags were weighed before and after being replaced to assure the accurate weight of fines generated in this time span. All samples and filter bags in the tests were weighed by a Mettler Toledo precision balance (ML3002), with a readability of 0.01 g. A slight tapping of the walls of the attrition chamber and settling chamber was conducted regularly.

2.4 Characterization of Attrition

The attrition resistance of granular material is generally characterized by the attrition index (AI) as defined in Eq. (1), being the percentage of the mass of fines less than 20 μm collected during the test in relation to the total mass of catalyst samples charged into the apparatus at the beginning of the test.

$$AI = \frac{m_{f20}}{m_0} \times 100 \qquad (1)$$

where m_{f20}[1)] is the mass of fines smaller than 20 μm, which is the sum of fines collected at each time interval during the whole test, and m_0 is the mass of catalyst samples initially charged to the apparatus.

The attrition mode is usually distinguished by comparing the PSDs of samples before and after the tests. After each test, the PSDs of particles remaining in the attrition chamber and fines collected at each time interval were analyzed. Eq. (2) defines the total PSD of the sample after the test including fines collected and the remaining particles in the attrition chamber.

$$PSD_{total} = \frac{\sum_{i,j} m_{i,j} PSD_{i,j} + m_r PSD_r}{\sum_{i,j} m_{i,j} + m_r} \qquad (2)$$

where $m_{i,j}$ is the mass of fines collected between the i-th and j-th hour, m_r is the mass of the remaining particles in the attrition chamber after each test, $PSD_{i,j}$ ($i < j$) is the PSD for fines collected between the i-th and j-th hour, and PSD_r is the PSD for the remaining particles in the attrition chamber.

The fine powder in the initial sample was removed before each test to ensure that the majority of fines collected by the filter bag were produced by attrition rather than that from the initial sample charged into the apparatus. It is clear that the

particle size will influence the fluidization performance, but the attrition of coarse particles might be more important in fluidized-bed operation as this is directly related to the catalyst lost in real units. Less than 1 wt % of initial catalyst particles charged into the reactor was lost after each of the experiments, which can be attributed to the fines elutriated in the feeding and unloading process.

3 Results and Discussion

3.1 Dependence of Attrition Index on Temperature

In Fig. 4, the attrition indices are plotted as function of temperature for all samples tested. A significant difference between the attrition indices of MTO and FCC catalysts can be found. Two stages can be clearly distinguished in terms of the influ-
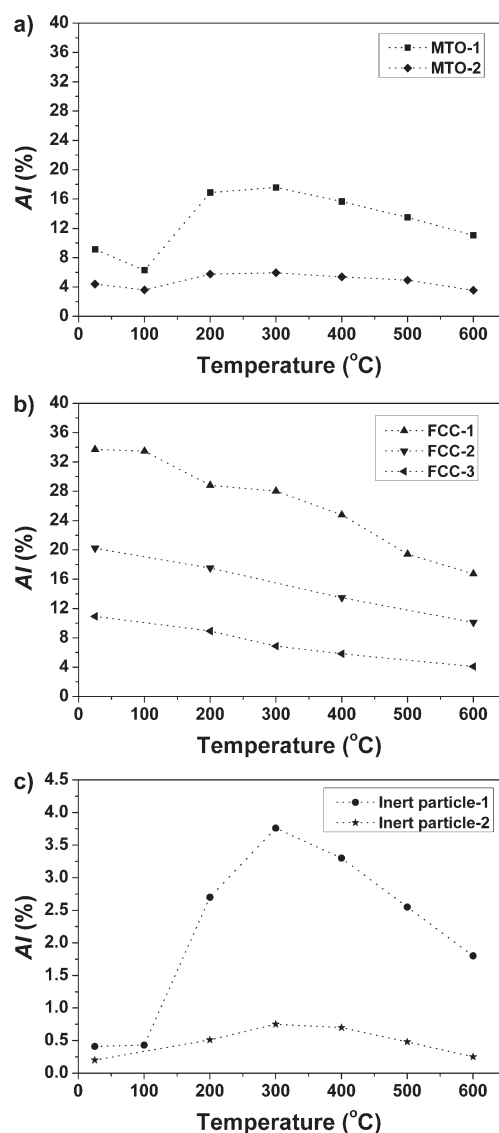

Figure 4. Attrition indices of samples from room temperature to 600 °C: (a) MTO-1, 2; (b) FCC-1, 2, 3; (c) inert particle-1, 2.

---

1)   List of symbols at the end of the paper.

ence of temperature on the attrition index of MTO catalyst particles. When the operation temperature increases, the attrition indices of MTO catalyst particles firstly rise and then drop significantly, reaching a maximum at around 300 °C (see Fig. 4 a), which suggests that the attrition rate of MTO catalyst particles has a complicated dependence on temperature.

The attrition performance of inert particles with temperature is illustrated in Fig. 4 c. Note that the catalyst attrition is related to mechanical, thermal, and chemical stress acting on the particles. In the current study, the chemical stress is not included. Concerning mechanical and thermal stress, the latter is mainly dominated by the material properties. MTO catalyst particles are composed of active components (SAPO-34 zeolites), binder, matrix, and additives, while the inert particles have almost identical compositions like MTO catalyst particles except SAPO-34 zeolites. According to Watanabe et al. [43] and Buchholz et al. [44], SAPO-34 zeolite is thermally stable at temperatures up to 900 °C, and no change of the crystallinity and microporous structure of the framework could be found at such high temperature. However, the material properties of the matrix, blinder, and additives, including the Young's modulus, brittleness, and surface energy, may vary at high temperature [38, 41, 45, 46]. Thus, it is expected the thermal resistance of MTO catalyst and inert particles has the similar trend with temperature, and consequently the attrition index has a similar shape. However, the mechanical stress of catalyst particles is strongly determined by the surface properties, inner structure, and among others. The much higher attrition index of MTO particles compared to the inert particles may be attributed to the existence of zeolite crystals in MTO particles. Without zeolite crystals inside, the inert particles have an amorphous inner structure. However, the MTO catalyst particles contain many crystals. The binding force at the interfaces between zeolite crystals and amorphous substance is relatively weak, thus lowers the strength of MTO catalyst particles.

From Fig. 4 b, it is obvious that the attrition indices of FCC catalyst particles drop monotonously with increasing operation temperature. This apparently deviates from that of MTO catalyst particles.

Chen et al. [36–38] studied the attrition of limestone in a circulating fluidized-bed combustor from 25 °C to 850 °C and found that the attrition index decreases with rising temperature. But Lin and Wey [34, 35] stated that the attrition of silica sand at high temperature in a bubble fluidized-bed incinerator exhibits a monotonous increase with operation temperature. Our results for FCC catalyst particles are consistent with the findings by Chen et al. [36–38] though the attrition indices of our MTO catalyst particles and inert particles manifest a maximum at 300 °C. This is certainly related to the material properties which may have a different dependence on temperature.

A quantitative explanation on the maximum attrition index of MTO catalyst and inert particles is dependent on the direct measurement of the material properties of powder at high temperature, which remains a big challenge so far. However, a hypothesis can be used to qualitatively explain this maximum attrition index. Note that the MTO catalyst particles consist of SAPO-34 zeolite, matrix, binder, and additives. As mentioned above, SAPO-34 zeolite has a good thermal stability [43, 44], and the material properties including hardness, Young's modu-

lus, brittleness etc. are closely related to temperature [38, 41, 45, 46]. Actually, as suggested by Werther and Reppenhagen, for any specified type of material there should be an optimal temperature range with respect to the attrition performance [4]. Thus, it can be argued that the material of nonactive components such as matrix, blinder, and additives of MTO catalyst particles has a weak attrition resistance in the temperature range around 300 °C. The existence of SAPO-34 zeolite crystals inside the catalyst does affect the mechanical stress but has a negligible influence on the thermal resistance. This also explains the similar maximum attrition index at around 300 °C for inert particles as the materials of inert particles are the same as those of the nonactive components in MTO catalyst particles.

A careful check with the experimental data suggests that the decrease of attrition index with rising temperature can be well described by:

$$AI(T) = AI_0 \exp[-k(T - T_0)] \tag{3}$$

where $AI(T)$ is the attrition index at temperature T, AI_0 is the pre-exponential factor, which can be influenced by the reactor layout and operation conditions, and among others, k is a constant rate that is only influenced by particle properties; T_0 means the characteristic temperature.

Tab. 3 lists the fitting parameters based on Eq. (3) for all samples. Fig. 5 compares the experimental with the prediction data based on Eq. (3). The attrition index of FCC catalyst particles can be well captured by Eq. (3). The attrition index of MTO catalyst particles at high temperature (> 300 °C) can also be predicted by Eq. (3). It should be stressed that, although Eq. (3) can provide a good representation for the attrition index of FCC and MTO catalysts at high temperature, it is not our intention to find a widely accepted formula. The parameters used in Eq. (3) would vary for different testing conditions.

Table 3. Fitting parameters of Eq. (3) for different samples.

Sample	T_0	A_0	k	R^2
MTO-1	300	17.82	0.00149	0.9857
MTO-2	300	6.11	0.00149	0.8918
FCC-1	25	36.19	0.00125	0.9307
FCC-2	25	20.94	0.00125	0.9809
FCC-3	25	10.30	0.00125	0.9207
Inert particle-1	300	3.97	0.00250	0.9490
Inert particle-2	300	0.78	0.00250	0.8506

3.2 Attrition Modes

The total PSDs of catalyst particles after tests at different temperatures are provided in Fig. 6. The PSDs measured at lower temperature, i.e., room temperature and 200 °C, have three peaks: the first one is around 100 μm, which follows exactly the mean size of the parent particles; the second one is in the range of 10–40 μm, showing debris with this size were generated due
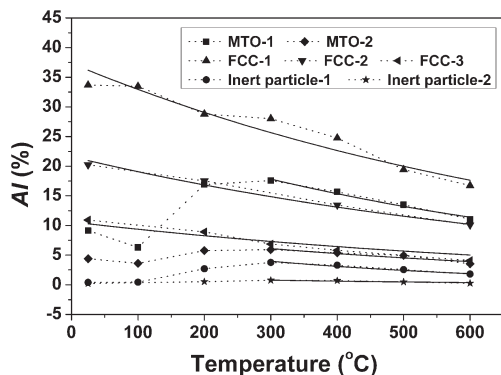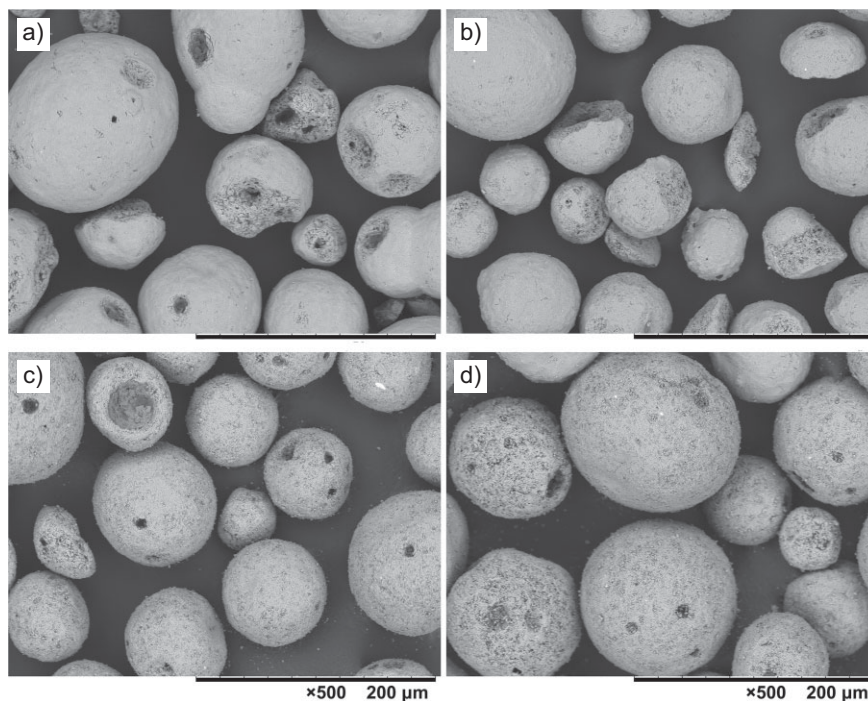
Figure 5. Dependence of attrition index on temperature for different samples. The solid lines are the fitting based on Eq. (3) and scatters denote experimental results.

to the fragmentation; and the third one is between 1 and 5 µm, indicating that the abrasion occurs at lower temperature, thus fines of 1–5 µm were found. Apparently, the attrition at lower temperature is a combination of abrasion and fragmentation. At high temperature, i.e., > 200–300 °C, only the first and third peaks remain in the PSDs of catalyst particles. This means that abrasion becomes the dominant attrition mode at high temperature.
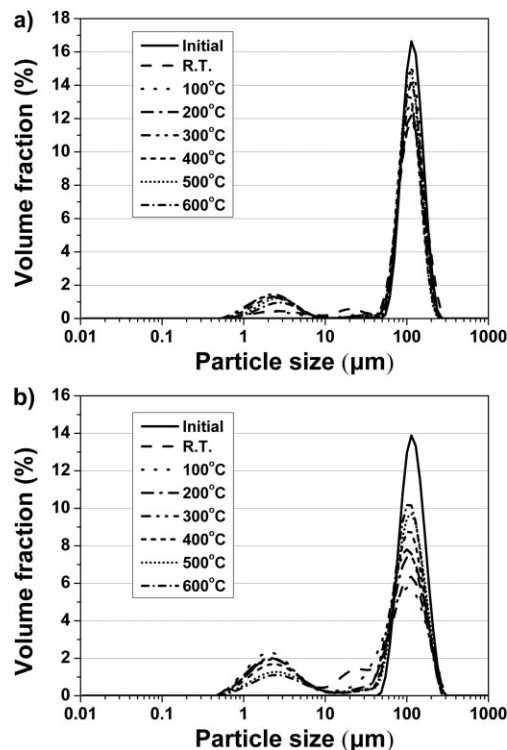
In Figs. 7 and Fig. S1 of Supporting Information, typical SEM photos of the MTO-1 and FCC-1 catalyst particles remaining in the reactor after attrition tests are presented. After the attrition tests at low temperature, i.e., at room temperature and 100 °C, small debris due to breakdown of the parent particles can be observed. The uneven shape of these debris evidenced that they were generated along the cracks on the parent particles (see Figs. 7 a, b and Fig. S1 a, b). After the attrition tests at higher temperature (200–600 °C), there are many superfine particles which generated by propagation of cracks on the particles' surface under the stress (see Figs. 7 c, d and Fig. S1 c, d, the SEM photos of 400–600 °C are similar). This agrees with the observation concerning the change of PSDs of catalyst particles.

3.3 Mechanism of Catalyst Attrition at High Temperature

As discussed above, the MTO catalyst particles have a better attrition resistance than FCC catalyst particles. However, the mechanism behind the different attrition performance between MTO and FCC catalysts with increasing temperature is not obvious. Werther and Reppenhagen [4] suggested that the attrition of catalysts at high temperature might be due to the thermal shock and the variation of particle and gas properties. At room temperature, the catalyst

Figure 6. Total PSDs of catalyst particles after tests: (a) MTO-1, (b) FCC-1.

particles are brittle and easy to break down into similar sizes because the cracks on the surface will develop readily. At high temperature, the material is softer than that at room temperature

Figure 7. SEM photos of MTO-1 after tests: (a) room temperature, (b) 100 °C, (c) 200 °C, (d) 300 °C.

and the particles become more resistant to the mechanical impact [18]. In this case, the chance for fragmentation is significantly reduced and abrasion is the main attrition mode.

The compositions of two catalysts are different. The molecular sieve of MTO is SAPO-34, and FCC is typically Y-type. The compositions of these two catalysts are compared in Tab. 2. The mechanical strength and attrition resistance performance of MTO and FCC catalyst particles depend on particle properties such as hardness, mechanical properties, and residual stress, which is eventually related to their compositions and the synthesis conditions. Another reason might be the initial shape and the cracks on the surface of these two catalyst particles. As can be seen in Fig. 3, the MTO catalyst particles have a much smoother surface than the FCC catalyst particles. Most of the MTO catalyst particles in the initial sample are spherical, with some small pieces sticking to the surface. The shapes of the FCC catalyst particles, however, deviate significantly from the perfect sphere, which certainly enhances the surface wear and thus abrasion of catalyst particles.

Also some cracks were found on the surface of FCC catalyst particles. The development of cracks on the catalyst surface is influenced by operation temperature, which may cause different attrition behavior at lower temperature. It has been found that porosity influences the stress distribution and cracks growth [47]. In addition, porosity affects the interfacial crack propagation of brittle materials [48]. As demonstrated in Fig. 8, the interior construction of MTO and FCC catalyst particles is different but both are porous and inhomogeneous. According to the study of Nakamura and Wang [49], the crack growth and propagation within inhomogeneous porous material is uneven and influenced by pore arrangements. In addition, the growth and propagation of the crack of porous materials at high temperature [50] is very complicated, which is influenced by the structure and composition of the material, environment temperature, and stress on the particles. In other words, these factors may partly contribute to the distinct attrition of MTO and FCC catalyst particles as the latter exhibits apparent cracks on the particle surface, as shown in Fig. S1.

It should be stressed that many factors will influence the attrition of catalyst particles, such as material properties, synthesis methods, and hydrodynamics in reactors. The attrition of catalyst particles is indeed a complicated process. However, as analyzed above, the compositions and surface cracks might play a key role in the distinct attrition behavior of MTO and FCC catalyst particles, especially at high temperature.

4 Conclusions

Although the design of the fluidized-bed reactors and the internals inside of the recently developed MTO process borrows a lot of experience from the FCC process, it has been found that the attrition of MTO catalyst particles is different from that of FCC catalyst particles at high temperature. In general, MTO catalyst particles have a better attrition resistance than FCC catalyst particles. The attrition index of FCC catalyst particles
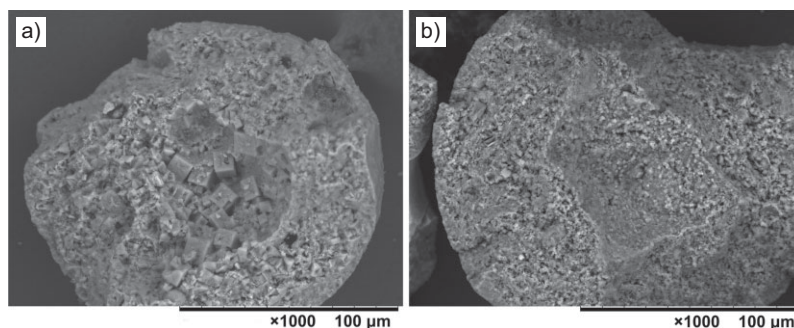

Figure 8. Interior morphology of catalyst particles: (a) MTO-1, (b) FCC-1.

shows a monotonous dependence on temperature, while that of MTO catalyst particles manifests a maximum at round 300 °C. An exponential relation was found which describes well the influence of temperature on the attrition index of MTO and FCC catalyst particles at high temperature.

Detailed analysis discovers that, among many complicated factors influencing the attrition of catalyst particles, the material composition and surface cracks would play the key role in the distinct attrition behavior. Both abrasion and fragmentation was found for either MTO or FCC catalyst particles at low temperatures, i.e., room temperature and 100 °C, while abrasion becomes the dominant attrition mode at high temperatures from 200 °C to 600 °C, which was confirmed by both PSD measurements and SEM of the samples. Although MTO catalyst particles have a lower attrition rate, most of fines generated are between 1 and 5 µm, which would be difficult to capture by multistage cyclones that are common practice in industrial MTO and FCC units. This should be taken into account in improving the cyclone design for MTO units.

Acknowledgment

Symbols used

AI	[%]	attrition index
$AI(T)$	[%]	attrition index at temperature T
AI_0	[–]	pre-exponential factor of Eq. (3)
d_{50}	[µm]	particle size
$D[3,2]$	[µm]	particle size
k	[–]	constant parameter of Eq. (3)
m_0	[g]	mass of catalyst samples initially charged to the apparatus
m_{f20}	[g]	mass of fines smaller than 20 µm
$m_{i,j}$	[g]	mass of fines collected between the i-th and j-th hour ($i < j$)
m_r	[g]	mass of the remaining particles in the attrition chamber after each test
$PSD_{i,j}$	[–]	PSD for fines collected between the i-th and j-th hour ($i < j$)

PSD$_r$	[–]	PSD for the remaining particles in the attrition chamber
PSD$_{total}$	[–]	total PSD of the sample after the test
T	[°C]	test temperature
T_0	[°C]	characteristic temperature

Subscripts

| i, j | [h] | attrition time |

Abbreviations

AI	attrition index
ASTM	American Society for Testing and Materials
FCC	fluid catalytic cracking
MTO	methanol-to-olefins
PSD	particle size distribution
SEM	scanning electron microscopy

References

[1] D. Geldart, *Powder Technol.* **1973**, *7 (5)*, 285–292. DOI: 10.1016/0032-5910(73)80037-3

[2] C. R. Bemrose, J. Bridgwater, *Powder Technol.* **1987**, *49 (2)*, 97–126. DOI: 10.1016/0032-5910(87)80054-2

[3] F. Scala, R. Chirone, P. Salatino, in *Fluidized Bed Technologies for Near-Zero Emission Combustion and Gasification* (Ed: F. Scala), Woodhead Publishing Limited, New York **2013**.

[4] J. Werther, J. Reppenhagen, in *Handbook of Fluidization and Fluid-Particle Systems* (Ed: W.-C. Yang), Marcel Dekker, New York **2003**.

[5] W. L. Forsythe, W. R. Hertwig, *Ind. Eng. Chem.* **1949**, *41 (6)*, 1200–1206. DOI: 10.1021/ie50474a015

[6] J. Wu et al., *J. Chin. Soc. Corros. Prot.* **2010**, *30 (2)*, 135–140.

[7] R. Boerefijn, N. J. Gudde, M. Ghadiri, *Adv. Powder Technol.* **2000**, *11 (2)*, 145–174. DOI: 10.1163/156855200750172286

[8] J. M. Whitcombe, I. E. Agranovski, R. D. Braddock, *Powder Technol.* **2003**, *137 (3)*, 120–130. DOI: 10.1016/j.powtec.2003.07.002

[9] J. Werther, J. Reppenhagen, *AlChE J.* **1999**, *45 (9)*, 2001–2010. DOI: 10.1002/aic.690450916

[10] S. A. Weeks, P. Dumbill, *Oil Gas J.* **1990**, *88 (16)*, 38–40.

[11] J. Reppenhagen, J. Werther, *Powder Technol.* **2000**, *113 (1–2)*, 55–69. DOI: 10.1016/s0032-5910(99)00290-9

[12] F. A. Zenz, *Hydrocarbon Process.* **1971**, *50 (2)*, 103–105.

[13] F. A. Zenz, *Hydrocarbon Process.* **1974**, *53 (4)*, 119–124.

[14] F. A. Zenz, E. G. Kelleher, *J. Powder Bulk Solids Technol.* **1980**, *4*, 13–20.

[15] D. Rong, M. Horio, *Int. J. Multiphase Flow* **2001**, *27 (1)*, 89–105. DOI: 10.1016/S0301-9322(00)00003-3

[16] H. Cui, P. Sauriol, J. Chaouki, *Chem. Eng. Sci.* **2003**, *58 (3–6)*, 1071–1077. DOI: 10.1016/s0009-2509(02)00649-8

[17] K. Svoboda, M. Hartman, *Ind. Eng. Chem. Process Des. Dev.* **1981**, *20 (2)*, 319–326. DOI: 10.1021/i200013a022

[18] J. Hao, Y. Zhao, M. Ye, Z. Liu, *Adv. Powder Technol.* **2015**, *26 (3)*, 734–741. DOI: 10.1016/j.apt.2015.03.010

[19] D. S. Kalakkad et al., *Appl. Catal., A* **1995**, *133 (2)*, 335–350. DOI: 10.1016/0926-860x(95)00200-6

[20] D. B. Bukur, V. Carreto-Vazquez, H. N. Pham, A. K. Datye, *Appl. Catal., A* **2004**, *266 (1)*, 41–48. DOI: 10.1016/j.apcata.2004.01.031

[21] T.-J. Lin, X. Meng, L. Shi, *Ind. Eng. Chem. Res.* **2012**, *51 (40)*, 13123–13131. DOI: 10.1021/ie3014428

[22] D. B. Bukur, W. P. Ma, V. Carreto-Vazquez, *Top. Catal.* **2005**, *32 (3–4)*, 135–141. DOI: 10.1007/s11244-005-2885-6

[23] R. Zhao et al., *Ind. Eng. Chem. Res.* **2001**, *40 (5)*, 1320–1328. DOI: 10.1021/ie0006458

[24] R. Zhao et al., *Ind. Eng. Chem. Res.* **2001**, *40 (4)*, 1065–1075. DOI: 10.1021/ie000644f

[25] J. J. Pis et al., *Powder Technol.* **1991**, *66 (1)*, 41–46. DOI: 10.1016/0032-5910(91)80079-x

[26] J. Tomeczek, P. Mocek, *AlChE J.* **2007**, *53 (5)*, 1159–1163. DOI: 10.1002/aic.11140

[27] M. Stein, J. P. K. Seville, D. J. Parker, *Powder Technol.* **1998**, *100 (2–3)*, 242–250. DOI: 10.1016/S0032-5910(98)00145-4

[28] L. Guo et al., *Chem. Eng. Technol.* **2014**, *37 (7)*, 1211–1219. DOI: 10.1002/ceat.201300306

[29] M. Arjmand et al., *Energy Fuels* **2015**, *29 (3)*, 1868–1880. DOI: 10.1021/ef502194s

[30] G. Azimi et al., *Int. J. Greenhouse Gas Control* **2015**, *34*, 12–24. DOI: 10.1016/j.ijggc.2014.12.022

[31] J. A. S. Cleaver, M. Ghadiri, N. Rolfe, *Powder Technol.* **1993**, *76*, 15–22.

[32] K. R. Yuregir, M. Ghadiri, R. Clift, *Chem. Eng. Sci.* **1987**, *42 (4)*, 843–853.

[33] M. Ghadiri et al., *Powder Technol.* **1991**, *65 (1–3)*, 311–320. DOI: 10.1016/0032-5910(91)80195-O

[34] C. L. Lin, M. Y. Wey, *Korean J. Chem. Eng.* **2003**, *20 (6)*, 1123–1130. DOI: 10.1007/bf02706947

[35] C. L. Lin, M. Y. Wey, *Korean J. Chem. Eng.* **2005**, *22 (1)*, 154–160. DOI: 10.1007/bf02701478

[36] Z. Chen, J. R. Grace, C. J. Lim, *Fuel* **2008**, *87 (7)*, 1360–1371. DOI: 10.1016/j.fuel.2007.06.012

[37] Z. Chen, J. R. Grace, C. J. Lim, *Powder Technol.* **2011**, *207 (1–3)*, 55–64. DOI: 10.1016/j.powtec.2010.10.010

[38] Z. Chen, C. J. Lim, J. R. Grace, *Chem. Eng. Sci.* **2007**, *62 (3)*, 867–877. DOI: 10.1016/j.ces.2006.10.022

[39] M. Hartman et al., *Chem. Pap.* **2013**, *67 (2)*, 164–172. DOI: 10.2478/s11696-012-0267-7

[40] F. Scala, A. Cammarota, R. Chirone, P. Salatino, *AlChE J.* **1997**, *43 (2)*, 363–373. DOI: 10.1002/aic.690430210

[41] F. Li, C. Briens, F. Berruti, J. McMillan, *Powder Technol.* **2012**, *228*, 385–394. DOI: 10.1016/j.powtec.2012.05.057

[42] ASTM D5757-11, ASTM **2011**.

[43] Y. Watanabe et al., *J. Catal.* **1993**, *143 (2)*, 430–436. DOI: 10.1006/jcat.1993.1287

[44] A. Buchholz et al., *Microporous Mesoporous Mater.* **2002**, *56 (3)*, 267–278. DOI: 10.1016/s1387-1811(02)00491-2

[45] W. B. Hillig, *J. Am. Ceram. Soc.* **1993**, *76 (1)*, 129–138. DOI: 10.1111/j.1151-2916.1993.tb03698.x

[46] H. L. Wang, M. H. Hon, *Ceram. Int.* **1999**, *25 (3)*, 267–271. DOI: 10.1016/S0272-8842(98)00035-2

[47] Y. Yang, Y. Ju, J. Chen, *J. China Coal Soc.* **2014**, *39 (4)*, 658–665.

[48] M. Dupeux, *J. Adhes. Sci. Technol.* **2011**, *25 (10)*, 1035–1048. DOI: 10.1163/016942410x524002

[49] T. Nakamura, Z. Wang, *J. Appl. Mech.* **2001**, *68 (2)*, 242–251. DOI: 10.1115/1.1356029

[50] A. Dobroskok, A. Ghassemi, A. Linkov, *Int. J. Fract.* **2005**, *134 (2)*, L29–L34. DOI: 10.1007/s10704-005-1369-9